Available online at www.sciencedirect.com
ScienceDirect
Acta Materialia 57 (2009) 4845–4854
Acta MATERIALIA
www.elsevier.com/locate/actamat

Effect of orientation on the cyclic deformation behavior of silver single crystals: Comparison with the behavior of copper and nickel single crystals

P. Li [a], Z.F. Zhang [a,*], X.W. Li [a,b], S.X. Li [a], Z.G. Wang [a]

[a] *Shenyang National Laboratory for Materials Science, Institute of Metal Research, Chinese Academy of Sciences, 72 Wenhua Road, 110016 Shenyang, China*

[b] *Institute of Materials Physics and Chemistry, College of Sciences, P.O. Box 104, Northeastern University, 110004 Shenyang, China*

Received 5 March 2009; received in revised form 5 June 2009; accepted 29 June 2009
Available online 28 July 2009

Abstract

This paper reports and discusses the effects of orientation on the cyclic deformation behavior of typical face-centered cubic (fcc) copper, nickel and silver single crystals, including the cyclic stress–strain (CSS) curves and dislocation configurations. Firstly, the CSS curves of silver single crystals of different orientations showed a clear plateau region over the strain range $\gamma_{pl} = 8.0 \times 10^{-5}$–$7.0 \times 10^{-3}$, however, there were two saturation shear stresses of 18–21 and 25–26 MPa, corresponding to the lower and upper plateau, respectively. After that, the dislocation configurations from differently oriented silver single crystals are well summarized as follows: (1) persistent slip band (PSB) ladders or walls appear in $[\bar{2}\,3\,9]$, $[0\,1\,1]$ and $[\bar{4}\,5\,9]$ silver single crystals; (2) a labyrinth is the main dislocation structure in the $[\bar{1}\,8\,1\,8]$ silver single crystal at high strain amplitudes; (3) vein and cell structures form in the $[\bar{2}\,3\,3]$ silver single crystal at low and high strain amplitudes, respectively; (4) interaction between the primary and secondary PSBs arises in the $[\bar{1}\,4\,1\,4]$ silver single crystal. Finally, combined with the results of copper and nickel single crystals, it can be concluded that the effects of orientation on the cyclic deformation behavior of these three kinds of single crystals follow a general principle. That is the orientation-dependent dislocation configuration can be divided into three regions in the stereographic triangle, including the central, $[0\,0\,1]$ and $[\bar{1}\,1\,1]$ regions.

Keywords: Silver single crystals; Orientation; Cyclic stress–strain curve; Dislocation configurations; Copper and nickel single crystals

1. Introduction

It is well known that one of the most important contributions in the cyclic deformation behavior of face-centered cubic (fcc) single crystals is the establishment of cyclic stress–strain (CSS) curve in single slip copper single crystals [1]. Mughrabi found that the CSS curve of copper single crystals at room temperature showed a clear plateau behavior with a plateau saturation stress of ~28 MPa over a wide range of plastic strain amplitudes from 6.0×10^{-5} to 7.5×10^{-3}. In region A, with $\gamma_{pl} \leq 6.0 \times 10^{-5}$, a vein structure is commonly seen. In plateau region B the plastic strain is mainly localized in narrow persistent slip bands (PSBs). In region C, with $\gamma_{pl} \geq 7.5 \times 10^{-3}$, the corresponding dislocation structure is composed of a labyrinth or cell. A two phase (PSBs and matrix) model was proposed to explain the distribution of plastic strain amplitude within PSBs and the matrix in fatigued copper single crystals [2,3].

Based on extensive experimental data from Mughrabi [1], Jin and Winter [4,5], Li et al. [6–9] and Gong et al. [10–12], Li et al. [13,14] summarized the plateau in the CSS curves of copper single crystals of different orientations. As shown in Fig. 1a, the CSS curves show significant differences with variations in orientation, which can be

* Corresponding author. Tel.: +86 24 23971043.
E-mail address: zhfzhang@imr.ac.cn (Z.F. Zhang).

1359-6454/$36.00 © 2009 Acta Materialia Inc. Published by Elsevier Ltd. All rights reserved.
doi:10.1016/j.actamat.2009.06.048

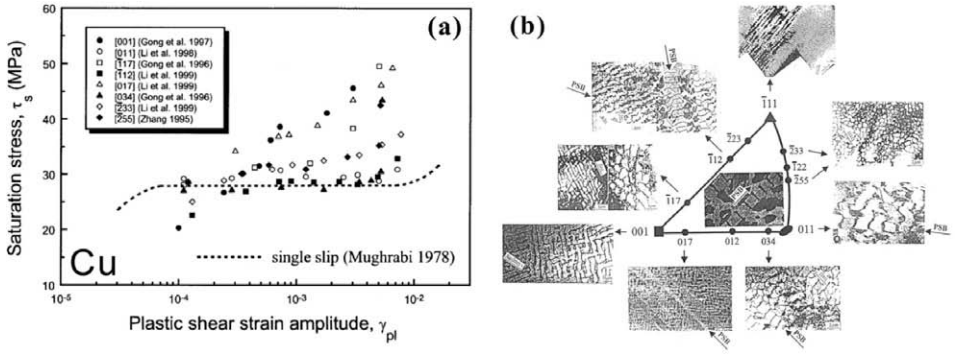

Fig. 1. CSS curves and dislocation configurations of copper single crystals with different orientations [13,14]. *Note:* Fig. 1b is drawn from extensive research [4–17].

specially introduced as follows: (1) a similar saturation plateau behavior is apparent for single, conjugate double and [0 1 1] multiple slip oriented copper single crystals; (2) co-planar double, critical double and [0 0 1] multiple slip oriented copper single crystals have higher CSS curves without plateau regions. The crystal orientations are usually summarized in the stereographic triangle. Different orientations have different slip systems. Firstly, for single slip oriented fcc single crystals the slip system should be $(1\,1\,1)[\bar{1}\,0\,1]$. Secondly, conjugate double slip systems include both $(1\,1\,1)[\bar{1}\,0\,1]$ and $(\bar{1}\,\bar{1}\,1)[0\,1\,1]$, co-planar double slip both $(1\,1\,1)[\bar{1}\,0\,1]$ and $(1\,1\,1)[\bar{1}\,1\,0]$, and critical double slip both $(1\,1\,1)[\bar{1}\,0\,1]$ and $(\bar{1}\,1\,1)[1\,0\,1]$. Finally, [0 1 1], $[\bar{1}\,1\,1]$ and [0 0 1] multiple slip oriented fcc single crystals have four, six and eight slip systems, respectively. Based on previous research [4–17], the dislocation configurations of copper single crystals with different orientations are illustrated in Fig. 1b. The classical PSB ladder structure appears in copper single crystals with single, conjugate double and [0 1 1] multiple slip orientations. As the orientations of copper single crystals change from [0 1 1] to [0 0 1] in the stereographic triangle the corresponding dislocation patterns vary from PSB ladders to a labyrinth structure. When the orientation changes from [0 1 1] to $[\bar{1}\,1\,1]$ PSB ladders will be gradually converted into a cell-like structure.

Orientation has a similar influence on the cyclic deformation behavior of nickel single crystals. Results from Bretschneider et al. [18] show that the CSS curve of nickel single crystals oriented for single slip is consistent with those of copper single crystals, apart from a higher saturation resolved shear stress (~50 MPa). Based on a comparison with the results of Bretschneider et al. [18] and Kahle [19], Buque et al. [20,21] systematically summarized the CSS curves and the classical dislocation configurations of nickel single crystals of different orientations. As shown in Fig. 2, there are also apparent plateau regions and classical PSB ladders in $[\bar{1}\,4\,9]$ and [0 1 1] nickel single crystals. However, a labyrinth structure appears in [0 0 1] nickel single crystals and a PSB wall structure forms in $[\bar{1}\,1\,1]$ nickel single crystals. As the orientation changes from $[\bar{1}\,4\,9]$ or [0 1 1] to [0 0 1] or $[\bar{1}\,1\,1]$ the CSS curve of nickel single crystals shows a continuous elevation and inclination, as a rule.

Systematic research has made it clear that the effect of orientation on the cyclic deformation behavior of copper and nickel single crystals is very similar. In addition, copper and nickel single crystals with the same orientation show a number of similar features, including CSS curves and dislocation patterns. Thus it would be interesting to determine how cyclic deformation behavior depends on orientation in the case of silver single crystals, another fcc metal. In previous works [22,23] some similarities in cyclic deformation behavior between copper and silver single crystals have been confirmed. The purpose of this study was to systematically summarize the cyclic deformation behavior of silver single crystals of different orientations

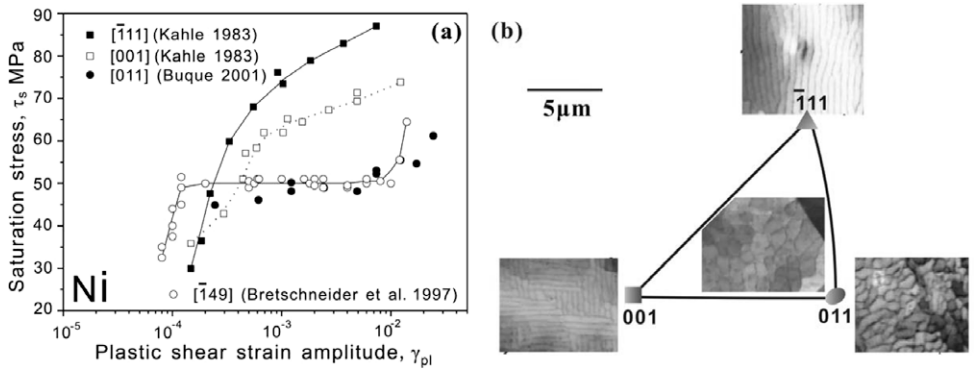

Fig. 2. CSS curves and dislocation configurations of nickel single crystals with different orientations. Courtesy of Buque [20,21].

and compare them with those of copper and nickel single crystals in order to obtain general principles concerning the effects of orientation on the cyclic deformation behavior of various fcc single crystals. Although the stacking fault energies (SFEs) of silver, copper and nickel are 16, 40 and 128 mJ m^{-2} [24], respectively, the three metals are similar so far as they all exhibit so-called wavy slip, indicating that cross-slip occurs easily.

2. Experimental procedures

To investigate the effect of orientation on the cyclic deformation behavior of silver single crystals bulk single crystal plates were firstly grown from electrolytic sliver of 99.999% purity by the Bridgman method. Secondly, fatigue specimens of $7 \times 5 \times 16$ mm gauge section and 54 mm total length were made using an electrospark cutting machine.

The crystal orientations of these specimens were determined by the electron back-scattering diffraction (EBSD) technique in a Cambridge S360 scanning electron microscope. All orientations of silver single crystals are illustrated in the stereographic triangle in Fig. 3. Cyclic deformation was performed in symmetric push–pull loading at room temperature in air using a Shimadzu servo-hydraulic testing machine. A triangular waveform signal with a frequency of 0.5 Hz was used for total strain control with the limitation of plastic strain. Plastic strain resolution and control precision were better than 10^{-5}. The peak loads in tension and compression and the hysteresis loops were recorded by computer automatically until cyclic saturation. After the fatigue tests all the fatigued specimens were carefully electro-polished and subsequently the dislocation configurations beneath the surface were carefully observed by the electron channeling contrast (ECC) technique in a Cambridge S360 scanning electron microscope. Such ECC images are similar in appearance to transmission electron micrographs, albeit with a lower image resolution [25–28]. However, the ECC technique has the great advantage of observation of fatigued dislocation patterns over a larger area, especially near grain boundaries, deformation bands or fatigue cracks [29–32].

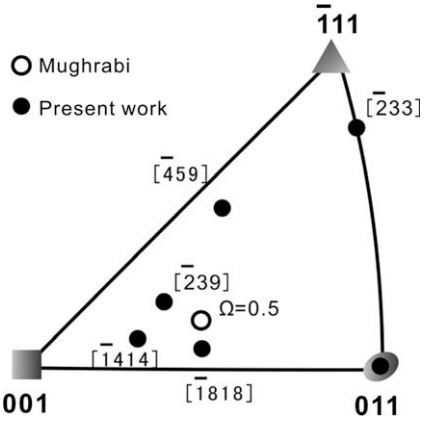

Fig. 3. Stereographic triangle showing the orientations of loading axis for silver single crystals in this paper. Open circles, single slip orientation with a Schmid factor $\Omega = 0.5$ [34,35]; filled circles, [233] and [239] [22,23].

3. Experimental results

For better comparison, Table 1 gives a survey of the specimens and the experiments performed, including the resolved shear stresses τ_s in saturation, the number of cycles N and the applied resolved shear strains γ_{pl}. The sample number corresponds to the plastic shear strain amplitude and the corresponding cycles. In Table 1 the selected orientations of the silver single crystals include [459], [1818], [1414] and [011]. In addition, data for [233] and [239] crystals in our previous studies [22,23] are also included. In this paper we will first compare the CSS curves of copper, nickel and silver single crystals with different orientations. Then the dislocation configurations of silver single crystals with the orientations listed above are compared. Finally, the effects of orientation on the CSS curves and dislocation configurations of copper, nickel and silver single crystals are discussed.

3.1. Cyclic hardening and saturation behavior

Several groups of cyclic hardening curves of silver single crystals with different orientations are shown in Fig. 4,

Table 1
Fatigue testing conditions and data for silver single crystals with different orientations.

Orientation	Specimen no.	γ_{pl}	Cyclic no.	τ_s (MPa)	Investigators
[233]	1	1.35×10^{-4}	20,000	24.5	Li et al. [22]
	2	6.7×10^{-4}	10,000	25.4	
	3	1.35×10^{-3}	5000	23.3	
	4	2.7×10^{-3}	4000	27.2	
	5	8.1×10^{-3}	2000	32	
[239]	1	2.1×10^{-3}	20,000	17.9	Li et al. [23]
[459]	1	1.15×10^{-3}	50,000	21.01	Present results
	2	2.3×10^{-3}	20,000	21.31	
	3	3.45×10^{-3}	15,000	22.71	
	4	4.6×10^{-3}	2500	24.53	
[1818]	1	1.0×10^{-3}	50,000	21.16	
	2	2.0×10^{-3}	20,000	21.2	
	3	4.0×10^{-3}	10,000	24.5	
	4	8.0×10^{-3}	8000	25.4	
[1414]	1	1.0×10^{-4}	50,000	23.2	
	2	1.5×10^{-4}	40,000	25.2	
	3	5.0×10^{-4}	20,000	26.6	
	4	1.0×10^{-3}	10,000	26.6	
	5	2.0×10^{-3}	4000	26.5	
	6	4.0×10^{-3}	3000	26.65	
	7	8.0×10^{-3}	2000	28.6	
[011]	1	1.5×10^{-4}	40,000	19	
	2	6.1×10^{-4}	20,000	19.4	
	3	3.7×10^{-3}	10,000	20.7	

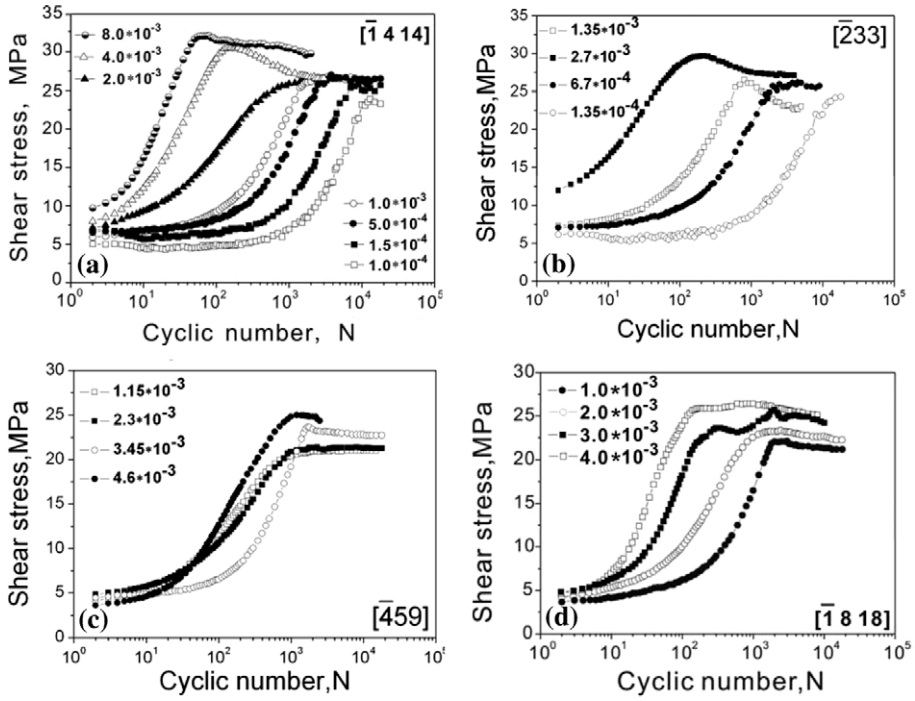

Fig. 4. Cyclic hardening curves of differently oriented silver single crystals at different strain amplitudes: (a) [1̄ 4 14] silver single crystals; (b) [2̄ 3 3] silver single crystals; (c) [4̄ 5 9] silver single crystals and (d) [1̄ 8 18] silver single crystals.

where the plotted resolved shear stresses are the mean values of the peak stresses in tension and compression [1]. Fig. 4 shows that no matter what the orientation, cyclic hardening was most pronounced in the early stages of cyclic deformation. After comparing the cyclic hardening curves of differently oriented silver single crystals the following conclusions can be drawn. (1) Under lower strain amplitudes ($\gamma_{pl} \leq 1.5 \times 10^{-3}$) the shear stress increased slowly with increasing cyclic number, finally developing a saturation state. As γ_{pl} increased and exceeded 2.0×10^{-3}, the hardening curves generally exhibited a clear stress overshoot and even secondary cyclic hardening could appear in [1̄ 8 18] silver single crystals. (2) Combined with the data in Table 1, the conclusion can be drawn that at the same strain amplitude the saturation resolved shear stresses of [1̄ 4 14] and [2̄ 3 3] silver single crystals are equivalent. Compared with them, the saturation shear stresses of [4̄ 5 9] and [1̄ 8 18] silver single crystals are obviously less than those of [1̄ 4 14] and [2̄ 3 3] silver single crystals.

3.2. Cyclic stress–strain (CSS) curves

It is well known that for single slip oriented copper single crystals the saturation plateau stress of the CSS curve is in the range 28–30 MPa [1–3,33]. For single slip oriented nickel single crystals the saturation shear stress in region B is ~50–52 MPa [18,34] (see Fig. 2). Thus, it would be interesting to determine whether there is a similar plateau region in silver single crystals and, if so, what is the corresponding saturation shear stress?

As shown in Fig. 5, the CSS curves were obtained by plotting all the obtained saturation stresses τ_s as a function of γ_{pl}, including the data from Mughrabi et al. [34,35]. For differently oriented silver single crystals it seems that all the data can be plotted as two curves with clear plateaux. One of the two plateaux is composed of data for [1̄ 4 14] and [2̄ 3 3] silver single crystals. The other plateau consists of the data for the orientations [2̄ 3 9], [4̄ 5 9], [1̄ 8 18] and [0 1 1], in combination with the CSS curve for the single slip oriented silver single crystals with a Schmid factor of $\Omega = 0.5$ [34,35]. Fig. 5 shows that the effect of orientation on the plateau stresses of silver single crystals is obvious. On the other hand, especially in the latter plateau, up to a shear strain amplitude of $\sim 1.0 \times 10^{-3}$ the saturation

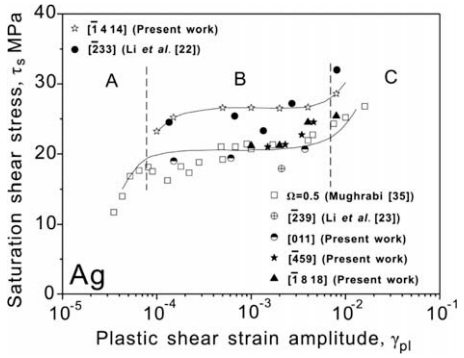

Fig. 5. CSS curves of differently oriented silver single crystals. The CSS curve data for silver single crystals with a Schmid factor $\Omega = 0.5$ are from unpublished work [35]. Courtesy of H. Mughrabi.

stresses are somewhat lower than at higher amplitudes. Therefore, it should be emphasized that the saturation stresses corresponding to the two plateaux are 18–21 and 25–26 MPa, respectively. Based on formation of the plateau, the CSS curves of silver single crystals can be divided into three regions: region A, $\gamma_{pl} \leq 8.0 \times 10^{-5}$; region B, $8.0 \times 10^{-5} \leq \gamma_{pl} \leq 7.0 \times 10^{-3}$; region C, $\gamma_{pl} \geq 7.0 \times 10^{-3}$. Similar to copper and nickel single crystals [1,18], the saturation shear stress τ_s increased with increasing γ_{pl} in regions A and C at low and high strain amplitudes, respectively. In the intermediate region B the CSS curve exhibits an extended plateau.

Finally, the CSS curves of fcc single crystals with single slip orientations, including copper, nickel and silver, are presented in Fig. 6. It can be concluded that the CSS curves of these three fcc single crystals with medium SFE, including copper, nickel and silver, often have three regions A, B and C. The three curves become gradually narrower from nickel to copper to silver and the corresponding plateau stresses become smaller in turn, from 50–52 to 28–30 to 18–21 MPa. In 1979 Mughrabi et al. [34] summarized the plateau stresses of the three metals and found that the characteristic thresholds for the formation of a PSB ladder structure at room temperature, expressed as τ_s/G, had a very similar value of 6.5×10^{-4} for the three kinds of single crystals, which is worth considering.

3.3. Typical dislocation patterns of silver single crystals with different orientations

3.3.1. Single slip orientations: $[\bar{2}\,3\,9]$ and $[\bar{4}\,5\,9]$

Fig. 7 shows the surface slip morphologies and the corresponding typical dislocation patterns of $[\bar{2}\,3\,9]$ silver single crystals at different magnifications. In Fig. 7a the slip bands (SBs) are distributed homogeneously in the specimen surface. Meanwhile, classical PSB ladders appear in $[\bar{2}\,3\,9]$ silver single crystals (see Fig. 7b), which correspond well with the surface SBs. At higher magnification the composition of the PSB ladder structure can be confirmed, called a rung [36]. In fact, it is clear that each PSB ladder is composed of a number of rungs with an equal interval distribution (see Fig. 7d). The first type of classical dislocation patterns, the PSB ladder, has been found in silver single crystals. Are the other dislocation configurations present?

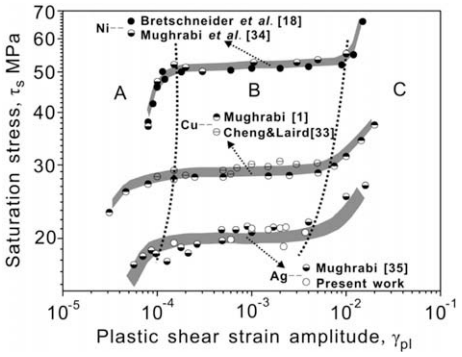

Fig. 6. CSS curves and their three regions of three fcc single crystals with a medium SFE, including copper, nickel and silver. The CSS curve data for silver single crystals are from present work and unpublished work [35]. Courtesy of H. Mughrabi.

Fig. 8 presents a PSB wall structure in $[\bar{4}\,5\,9]$ silver single crystals. PSB walls are also one of the classical dislocation configurations in fatigued copper and nickel single crystals [20,31]. These walls are approximately perpendicular to the primary Burgers vector and to the primary slip plane and they lie approximately on the $(\bar{1}\,0\,1)$ plane. Figs. 7 and 8 show that in the plateau region of silver single crystals with a single slip orientation the plastic strain is still mainly localized in narrow PSBs, composed of PSB ladders or PSB walls, as it is in copper and nickel single crystals with a single slip orientation.

3.3.2. Double slip orientations: $[\bar{1}\,8\,18]$, $[\bar{1}\,4\,14]$ and $[\bar{2}\,3\,3]$

The dislocation configurations of single slip oriented silver single crystals have been described above. Here, the typical dislocation patterns of double- slip or near double slip oriented silver single crystals will be introduced. First, $[\bar{1}\,8\,18]$ silver single crystals will be considered. As shown in Fig. 9, changes in dislocation configuration can be clearly observed with increasing strain amplitude. When $\gamma_{pl} = 1.0 \times 10^{-3}$ a PSB ladder structure started to appear. However, most PSB ladders only became clear at a strain amplitude of $\gamma_{pl} = 2.0 \times 10^{-3}$ (see Fig. 9b). As the strain amplitude increased to 4.0×10^{-3} PSB ladders corresponding to secondary SBs also appeared in the specimen surface, with two sets of PSB ladders interlaced with each other. On further increasing the strain amplitude to 8.0×10^{-3} the dislocation patterns became dominated by a labyrinth structure. The effect of strain amplitude on the dislocation configurations in $[\bar{1}\,8\,18]$ silver single crystals can be understood as that for single slip oriented copper single crystals [37]. Thus, although the orientation of $[\bar{1}\,8\,18]$ silver single crystals is closer to critical double slip ones, they behave like single slip oriented ones.

The influence of the number of cycles on dislocation configuration was primarily studied for $[\bar{1}\,4\,14]$ silver single crystals. Fig. 10 shows that interactions between primary and secondary PSB ladders still play an important role during cyclic deformation although the primary and secondary PSB ladders have their respective regions (see Fig. 10d). Meanwhile, it was found that with increasing cycle number the proportion between primary and secondary PSB regions gradually changed from a structure dominated by primary PSB regions to a structure with an equal proportion of primary and secondary ones. $[\bar{2}\,3\,3]$ silver single crystals have a co-planar double slip orientation. In previous research on $[\bar{2}\,3\,3]$ copper single crystals Li et al. [6,14] found that its CSS curve showed a quasi-plateau and the saturation stress did not increase remarkably with increasing γ_{pl} in the range 3.0×10^{-4}–2.3×10^{-3}. The corresponding saturation stress was 4–5 MPa higher than that of single slip oriented copper single crystals (see Fig. 1a).

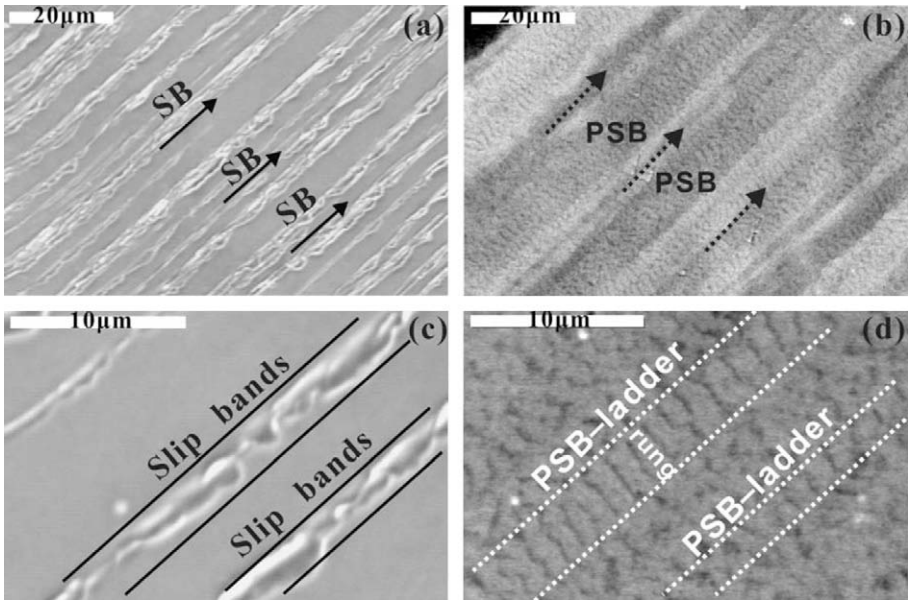

Fig. 7. Surface slip morphologies and dislocation patterns of $[\bar{2}\,3\,9]$ silver single crystals at a plastic strain amplitude of $\gamma_{pl} = 2.1 \times 10^{-3}$: (a and c) surface slip morphologies; (b and d) PSB ladder structures. Viewed from $(1\,\bar{2}\,1)$.

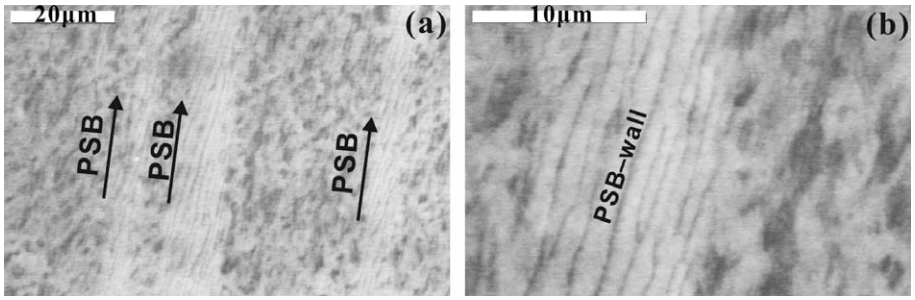

Fig. 8. Dislocation patterns of $[\bar{4}\,5\,9]$ silver single crystals under different magnifications at a plastic strain amplitude of $\gamma_{pl} = 4.6 \times 10^{-3}$: (a) PSBs and (b) PSB wall structure. Viewed from $(1\,\bar{1}\,1)$.

From Fig. 1b it can be found that the dislocation configurations of $[\bar{2}\,3\,3]$ copper single crystals are dominated by a cell structure. Likewise, a cell structure also appears in fatigued $[\bar{2}\,3\,3]$ silver single crystals. As shown in Fig. 11a, for $[\bar{2}\,3\,3]$ silver single crystals at low strain amplitude a dislocation vein microstructure can be clearly seen. With increasing γ_{pl} the specimen surface consists entirely of cell structure (see Fig. 11b), which further demonstrates that orientation must play an important role in the cyclic deformation behavior of silver single crystals.

3.3.3. Multiple slip orientation: [0 1 1]

The multiple slip orientations have their own features. Here we will mainly deal with [0 1 1] multiple slip oriented silver single crystals. Li et al. [9] and Buque [20] systematically summarized the cyclic deformation behavior of [0 1 1] copper and nickel single crystals, respectively. Comparing the results in Figs. 1 and 2, it is interesting to note that the CSS curves of [0 1 1] single crystals, of both copper and nickel, are approximately in accordance with those of single slip oriented ones. On the other hand, the classical PSB ladder structure also appears in both copper and nickel [0 1 1] single crystals. Thus it will be interesting to see how [0 1 1] silver single crystals behave.

Fig. 12 presents typical dislocation patterns for [0 1 1] silver single crystals at a plastic strain amplitude of $\gamma_{pl} = 6.1 \times 10^{-4}$. It can be seen that PSB wall and PSB ladder structures appear simultaneously in the specimen. As shown in Fig. 12a, regular dislocation walls form within DBs. Similar configurations also appear in copper and nickel single crystals [20,31]. Zhang et al. [31] defined these DBs with parallel dislocation walls as well-developed DBs. The wall structure in [0 1 1] silver single crystals is different from that in $[\bar{4}\,5\,9]$ silver single crystals. Compared with Fig. 8, it can be seen that the wall structure in [0 1 1] silver single crystals is mainly located in DBs, with a two phase structure composed of PSBs and veins on both sides of the DBs. However, the PSB wall structure in $[\bar{4}\,5\,9]$ silver single crystals is not located in DBs. The walls themselves correspond to SBs, thus there is only vein structure on both

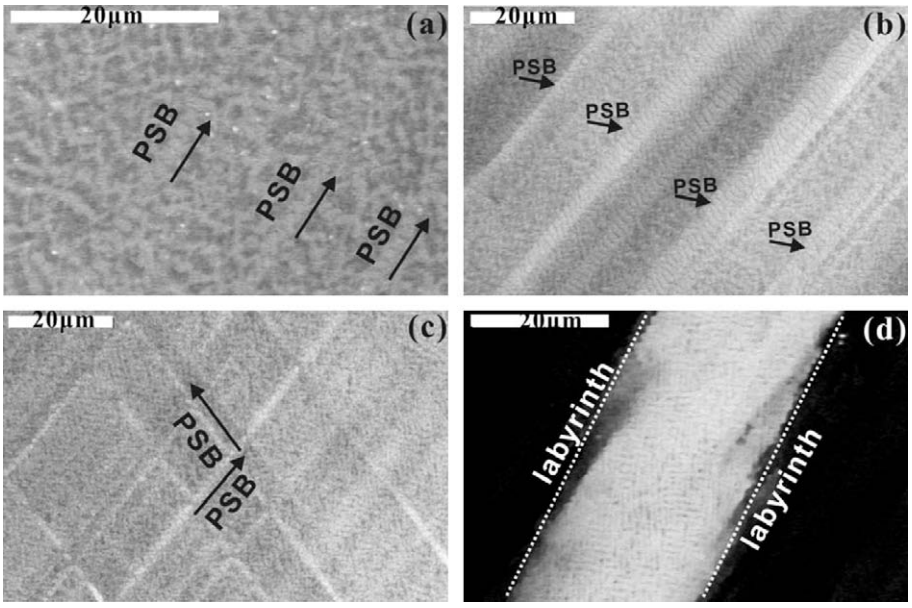

Fig. 9. Dislocation structures of $[\bar{1}\,8\,18]$ silver single crystals at different plastic strain amplitudes: (a) $\gamma_{pl} = 1.0 \times 10^{-3}$; (b) $\gamma_{pl} = 2.0 \times 10^{-3}$; (c) $\gamma_{pl} = 4.0 \times 10^{-3}$ and (d) $\gamma_{pl} = 8.0 \times 10^{-3}$. Viewed from $(2\bar{2}1)$.

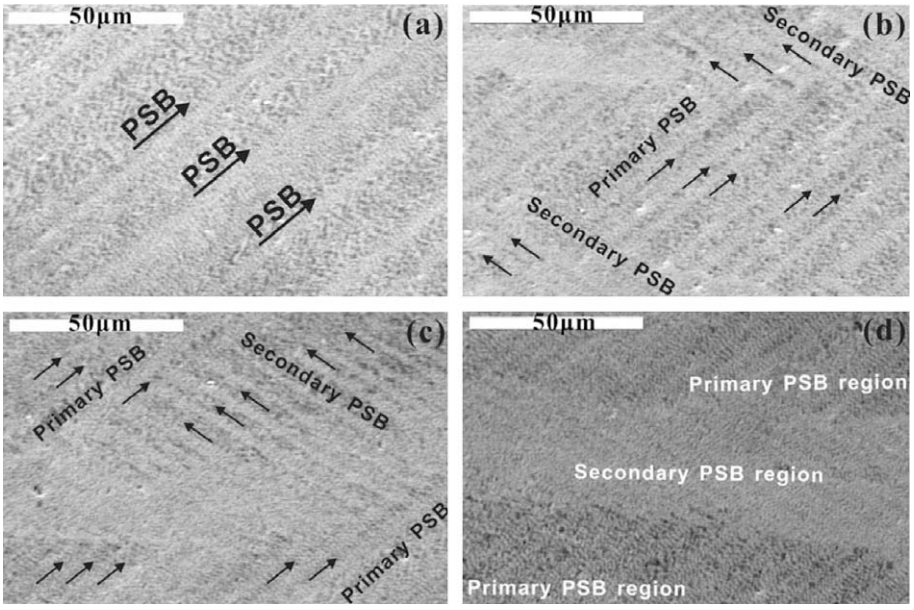

Fig. 10. Dislocation structures of $[\bar{1}\,4\,14]$ silver single crystals after different numbers of cycles at a plastic strain amplitude of $\gamma_{pl} = 5.0 \times 10^{-4}$: (a) 3000 cycles; (b) 5000 cycles; (c) 10,000 cycles and (d) 20,000 cycles. Viewed from $(6\bar{2}1)$.

sides of the walls. In addition, PSB ladders are the other major dislocation structure in [0 1 1] silver single crystals. Fig. 12d shows a classical PSB ladder structure, but in which the rungs are not as regular as those in PSB ladders in $[\bar{2}\,3\,9]$ silver single crystals, compared with Fig. 7d. In the same way, Buque [20] found that a PSB ladder structure with irregular rungs appeared in [0 1 1] nickel single crystals. Although the dislocation structure was slightly different, it did not affect the similarity between [0 1 1] and single slip oriented single crystals, including copper, nickel and silver.

4. Discussion

4.1. Effect of orientation on dislocation patterns of silver single crystals

From the observations above it can be seen that there are big differences in the dislocation patterns in silver single crystals with different orientations. Thus, an interesting question arises. Does the effect of orientation follow certain laws? The results for silver single crystals are shown in Fig. 13. Similar to copper and nickel single crystals (see

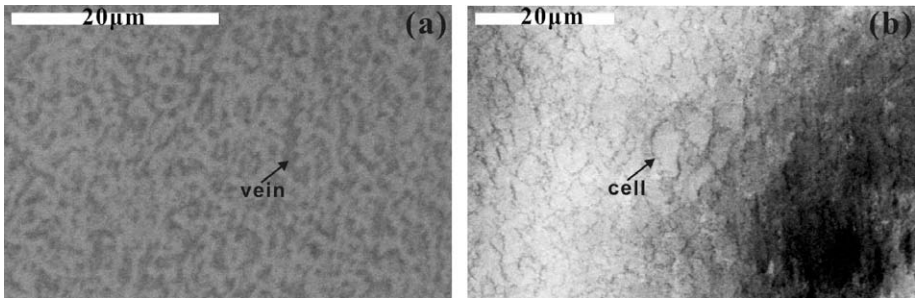

Fig. 11. Dislocation configurations of $[\bar{2}\,3\,3]$ silver single crystals: (a) vein at a plastic strain amplitude of $\gamma_{pl} = 1.35 \times 10^{-4}$ and (b) cell at a plastic strain amplitude of $\gamma_{pl} = 8.1 \times 10^{-3}$. Viewed from $(3\,3\,\bar{1})$.

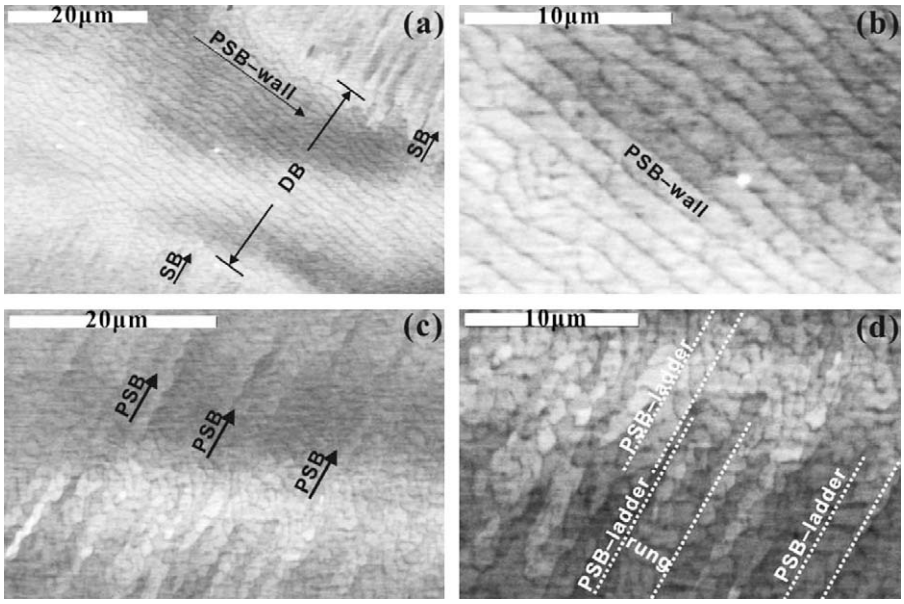

Fig. 12. Dislocation patterns of [0 1 1] silver single crystals at different magnifications at a plastic strain amplitude of $\gamma_{pl} = 6.1 \times 10^{-4}$; (a and b) PSB wall structure; (c and d) PSB ladder structure. Viewed from $(2\,\bar{1}\,1)$.

Figs. 1b and 2b), the typical PSB ladder structure also appears in single slip oriented silver single crystals. However, in $[\bar{4}\,5\,9]$ silver single crystals near the $0\,0\,1/\bar{1}\,1\,1$ side the typical dislocation structure is PSB walls. Such a wall structure can also be regarded to some extent as a PSB ladder one. Looking at the bottom of the stereographic triangle, in $[\bar{1}\,4\,14]$ and $[\bar{1}\,8\,18]$ silver single crystals close to the $0\,0\,1/0\,1\,1$ side the typical dislocation configurations are dominated by primary PSBs or an interaction between primary and secondary PSBs. On occasion, a labyrinth structure can also appear. In [0 1 1] multiple slip oriented silver single crystals PSB ladders or walls are the major dislocation patterns, analogous to those in single or conjugate double slip oriented silver single crystals. Finally, in $[\bar{2}\,3\,3]$ silver single crystals on the $0\,1\,1/\bar{1}\,1\,1$ side a vein structure is present. At higher strain amplitudes a cell-like structure can also form, however, no matter how high the strain amplitude, no classical PSB ladder structure was found.

The above laws are closely associated with the CSS curves of silver single crystals. Combined with Fig. 5, it can be seen that classical PSB ladder or PSB wall structures always appear in region B of the CSS curve, which corresponds to the occurrence of a plateau behavior. Formation of labyrinth and cell structures occurs in region C. Only in those silver single crystals with orientations near [0 0 1] or $[\bar{1}\,1\,1]$ such dislocation structures are formed more easily.

4.2. Effect of orientation on cyclic deformation of fcc single crystals with medium SFE

Fig. 14a presents the principles of the effect of orientation on plateau behavior, as summarized by Li et al. [13]. It can be seen that in the interior of the stereographic triangle single slip oriented copper single crystals show classical plateau behavior [1]. Next, attention is turned to the three vertexes. In [0 0 1] and $[\bar{1}\,1\,1]$ copper single crystals no plateau region is apparent [12,38], however, in [0 1 1] copper single crystals obvious plateau behavior can be found. On the three sides of the stereographic triangle Li et al. [13] found that the following rules apply. On the $0\,0\,1/\bar{1}\,1\,1$ side

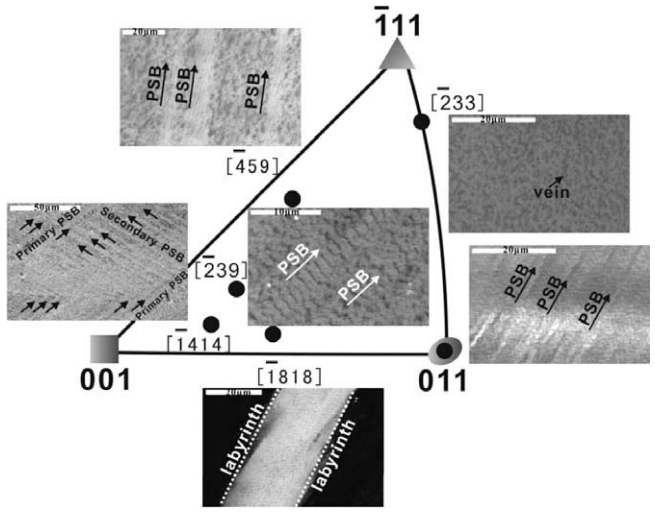

Fig. 13. Effect of the orientation on the dislocation patterns of silver single crystals.

[8], considering [$\bar{1}$ 1 2] as the center, an orientation transition to [0 0 1] and [$\bar{1}$ 1 1] results in a gradual change in the CSS curves from an obvious plateau to no plateau. On the 0 0 1/0 1 1 side [7], in transition from [0 1 1] to [0 0 1] the CSS curves change from clear plateau to shorter plateau to quasi-plateau to no plateau. On the 0 1 1/$\bar{1}$ 1 1 side [6], from the wide plateau of [0 1 1] copper single crystals to no plateau for [$\bar{1}$ 1 1] copper single crystals, the quasi-plateau behavior of co-planar double slip oriented copper single crystals can be regarded as a transition.

Through the above analysis the effect of orientation on plateau behavior has been elucidated. It is known that copper, nickel and silver crystals exhibit many similarities in the cyclic deformation behavior. The effect of orientation on the dislocation configurations of fcc single crystals with medium SFE are summarized in Fig. 14b. The CSS curves and dislocation configurations of [1 1 2] and [0 1 1] single crystals, whether copper, nickel or silver, are approximately the same for the whole stereographic triangle, thus the connection line segment between the [$\bar{1}$ 1 2] and [0 1 1] orientations can be considered a symmetry axis and the [0 0 1] and [$\bar{1}$ 1 1] orientations as extreme points. In this way the whole stereographic triangle can be divided into three regions: a central region, the [0 0 1] region and the [$\bar{1}$ 1 1] region. The central region is composed of most single slip orientations, a number of the conjugate double slip orientations and the [0 1 1] orientation. Their common characteristics are the formation of plateaux and PSB adder or wall structures. The [0 0 1] region is made up of orientations around the [0 0 1] orientation, including itself. The common features are no plateau and a labyrinth structure as their final saturation dislocation configuration. The [$\bar{1}$ 1 1] region is composed of orientations around the [$\bar{1}$ 1 1] orientation, including itself. The common characteristics are no plateau and a vein structure at low strain amplitudes with a cell or wall structure at high strain amplitudes as the dislocation patterns [39]. It can be said that the impact of orientation on dislocation structure may follow the same principles, however, this requires further research.

5. Conclusions

Copper, nickel and silver are three typical fcc metals. It is worth systematically considering the cyclic deformation behavior of their single crystals. Based on CSS curves and dislocation configurations of typical single crystals with various orientations, the following conclusions can be drawn.

1. Differently oriented silver single crystals show two clear plateaux in their CSS curves over the strain amplitude range $\gamma_{pl} = 8.0 \times 10^{-5}$–$7.0 \times 10^{-3}$. One is composed of data for [$\bar{1}$ 4 14] and [$\bar{2}$ 3 3] silver single crystals, while the other consists of data from other orientation silver single crystals. The two plateau stresses are 18–21 and 25–26 MPa, respectively.

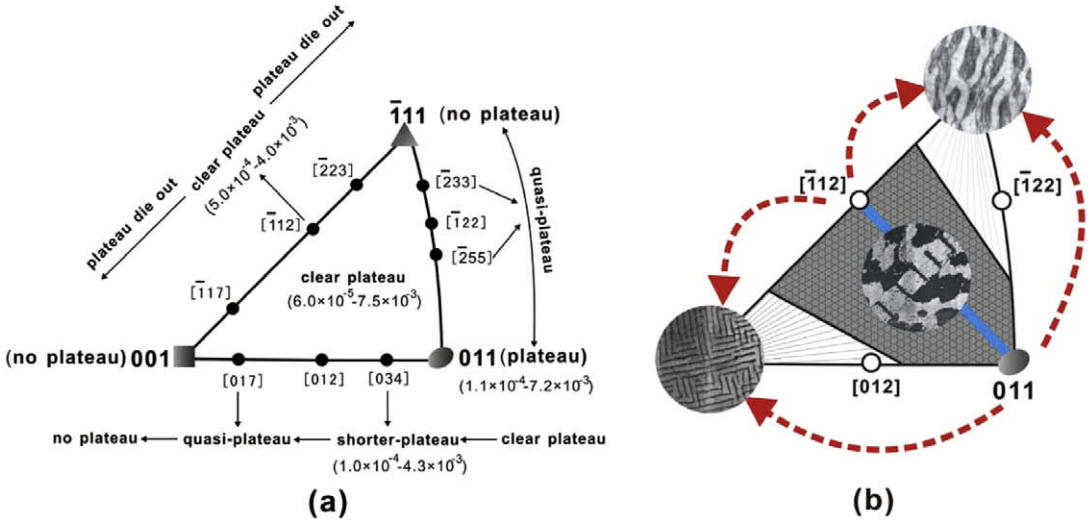

Fig. 14. Effect of orientation on the cyclic deformation of fcc single crystals: (a) Effect of the orientation on the CSS curves of copper single crystals [13] and (b) general principles concerning the effect of the orientation.

2. Different dislocation configurations appear in differently oriented silver single crystals. PSB ladders or walls appear in $[\bar{2}\,3\,9]$, $[0\,1\,1]$ and $[\bar{4}\,5\,9]$ silver single crystals in the saturation plateau region. A labyrinth structure is formed in $[\bar{1}\,8\,1\,8]$ silver single crystals at high strain amplitudes. Veins and cells are the main structures in $[\bar{2}\,3\,3]$ silver single crystals at low and high strain amplitudes, respectively. Interaction between the primary and secondary PSBs appears in $[\bar{1}\,4\,1\,4]$ silver single crystal.
3. Combined with the results for copper and nickel single crystals, the effects of orientation on the cyclic deformation behavior of the three typical single crystals is found to follow general principles: the effect of orientation on cyclic deformation and dislocation configurations can be divided into three regions in the stereographic triangle, including a central region, the $[0\,0\,1]$ region and the $[\bar{1}\,1\,1]$ region.

Acknowledgments

The authors are grateful to Prof. H. Mughrabi for providing us with unpublished data on the cyclic stress–strain curve of silver single crystals. Thanks are also due to H.H. Su, W. Gao, P. Zhang and H.F. Zou for their assistance in the fatigue experiments, slip morphology and dislocation observations. This work was financially supported by the Hundreds of Talents Project of Chinese Academy of Sciences, the National Outstanding Young Scientist Foundation (Z.F. Zhang) under Grant No. 50625103, and the National Natural Science Foundation of China (X.W. Li) under Grant No. 50771029. Z.F. Zhang would like to acknowledge the financial support by National Basic Research Program of China under Grant No. 2010CB631006.

References

[1] Mughrabi H. Mater Sci Eng 1978;33:207–23.
[2] Winter AT. Philos Mag 1974;30:719–38.
[3] Finney JM, Laird C. Philos Mag 1975;31:339–66.
[4] Jin NY. Philos Mag 1983;48:L33–8.
[5] Jin NY, Winter AT. Acta Metall 1984;32:989–95.
[6] Li XW, Wang ZG, Li SX. Mater Sci Eng 1999;A260:132–8.
[7] Li XW, Wang ZG, Li SX. Mater Sci Eng 1999;A265:18–24.
[8] Li XW, Wang ZG, Li SX. Mater Sci Eng 1999;A269:166–74.
[9] Li XW, Wang ZG, Li GY, Wu SD, Li SX. Acta Mater 1998;46:4497–505.
[10] Gong B, Wang ZG, Zhang YW. Mater Sci Eng 1995;A194:171–8.
[11] Gong B, Wang ZR, Wang ZG, Zhang YW. Mater Sci Eng 1996;A210:94–101.
[12] Gong B, Wang ZR, Wang ZG. Acta Mater 1997;45:1365–77.
[13] Li XW, Wang ZG, Li SX. Philos Mag Lett 1999;79:715–9.
[14] Li XW, Zhang ZF, Wang ZG, Li SX, Umakoshi Y. Defect Diffus Forum 2001;188–190:153–70.
[15] Wang ZG, Zhang ZF, Li XW, Jia WP, Li SX. Mater Sci Eng 1996;A319–321:63–73.
[16] Lepisto TK, Kuokkala VT, Kettunen PO. Scripta Metall 1984;18:245–8.
[17] Lepisto TK, Kuokkala VT, Kettunen PO. Mater Sci Eng 1986;81:457–63.
[18] Bretschneider J, Holste C, Tippelt B. Acta Mater 1997;45:3775–83.
[19] Kahle E. Untersuchungen zur Stabilitat bei zyklisch verformten Nickel- und Nickel–Kobalt-Einkristalle. Ph.D. thesis, Technical University of Dresden; 1983.
[20] Buque C. Int J Fatigue 2001;23:671–8.
[21] Buque C, Bretschneider J, Schwab A, Holste C. Mater Sci Eng 2001;A300:254–62.
[22] Li P, Zhang ZF, Li SX, Wang ZG. Acta Mater 2008;56:2212–22.
[23] Li P, Zhang ZF, Li SX, Wang ZG. Scripta Mater 2008;59:730–3.
[24] Wang ZR. Philos Mag 2004;84:351–79.
[25] Zauter R, Petry F, Bayerlein M, Sommer C, Christ HJ, Mughrabi H. Philos Mag 1992;66:425–36.
[26] Schwab A, Bretschneider J, Buque C, Blochwitz C, Holste C. Philos Mag Lett 1996;74:449–54.
[27] Melisova D, Weiss B, Stickler R. Scripta Mater 1997;36:1061–6.
[28] Ahmed J, Wilkinson AJ, Roberts SG. Philos Mag 2001;A81:1473–88.
[29] Zhang ZF, Wang ZG. Philos Mag Lett 1998;78:105–13.
[30] Zhang ZF, Wang ZG, Hu YM. Scripta Mater 1999;40:1353–8.
[31] Zhang ZF, Wang ZG, Sun ZM. Acta Mater 2001;49:2875–86.
[32] Zhang ZF, Wang ZG. Acta Mater 2003;51:347–64.
[33] Cheng AS, Laird C. Mater Sci Eng 1981;51:111–21.
[34] Mughrabi H, Ackermann F, Herz K. In: Fong JT, editor. Fatigue mechanisms. ASTM STP 675. Philadelphia: ASTM; 1979. p. 69–105.
[35] Mughrabi H. Unpublished data of 1979. Private communication; 2008.
[36] Winter AT. Philos Mag 1973;28:57–64.
[37] Ackermann F, Kubin LP, Lepinoux J, Mughrabi H. Acta Metall 1984;32:715–25.
[38] Lepisto TK, Kettunen PO. Mater Sci Eng 1986;83:1–15.
[39] Li XW, Zhou Y, Guo WW, Zhang GP. Cryst Res Technol 2009;44:315–21.